

Supplement:

Organic sulfur fluxes and geomorphic control of sulfur isotope ratios in rivers

Preston C. Kemeny^{a*}, Mark A. Torres^b, Michael P. Lamb^a, Samuel M. Webb^c, Nathan Dalleska^a, Trevor Cole^b, Yi Hou^b, Jared Marske^a, Jess F. Adkins^a, Woodward W. Fischer^a

^a Geological and Planetary Sciences, California Institute of Technology, Pasadena, CA, USA

^b Earth, Environmental, and Planetary Sciences, Rice University, Houston, TX, USA

^c Stanford Synchrotron Radiation Lightsource, SLAC National Accelerator Laboratory, Menlo Park, CA, USA

*Corresponding author: pkemeny@caltech.edu, preston.kemeny@gmail.com

Appendices

Appendix A: Images of the Efri Haukadalsá catchment	page 2
Appendix B: Chromatography measurements of cation concentration	page 5
Appendix C: Synchrotron filter blank and vegetation mapping	page 7
Appendix D: Seasonality of precipitation	page 9
Appendix E: River inversion model with Monte Carlo error propagation.....	page 15
Appendix F: Extended geomorphic analysis.....	page 20
Appendix G: Additional maps of dissolved chemistry	page 21
Appendix H: Chemostatis in the Efri Haukadalsá	page 22
Appendix I: Temporal changes in Haukadalsvatn chemistry	page 24
Appendix J: Rayleigh model for sediment $\delta^{34}\text{S}$	page 25
References:	page 27

Tables

Table E.1: End-member distributions for Monte Carlo inversion model	page 17
Table H.1: Dissolved chemistry of repeat river water samples across field seasons	page 23

Figures

Fig. A.1: Drone images of the Efri Haukadalsá catchment	page 2
Fig. A.2: Field photographs of the Efri Haukadalsá catchment	page 3
Fig. A.3: Satellite images of the Efri Haukadalsá catchment	page 4
Fig. B.1: $[\text{Ca}^{2+}]$, $[\text{Mg}^{2+}]$, $[\text{Na}^+]$, $[\text{K}^+]$ determinations	page 6
Fig. C.1: Synchrotron analysis of vegetation cross section	page 8
Fig. D.1: Seasonal changes in precipitation, wind speed at Ásgarður and Stykkishólmur ..	page 11
Fig. D.2: Seasonal changes in precipitation chemistry at Íráfoss and Stórhöfði	page 12
Fig. D.3: Sulfur mixing diagram, $\delta^{34}\text{S}_{\text{SO}_4}$ against $\text{Cl}^-/\text{SO}_4^{2-}$ with inversion end-members...	page 13
Fig. D.4: Seasonal $\delta^{34}\text{S}_{\text{SO}_4}$ and $\text{Cl}^-/\text{SO}_4^{2-}$ in Hvítá, Olfusa, Thjorsa, and Sog Rivers.....	page 14
Fig. E.1: Inversion results for the fractional contributions of end-members	page 18
Fig. E.2: Inversion results with & without carbonate for variable precipitation	page 19
Fig. F.1: Extended geomorphic analysis	page 20
Fig. G.1: $[\text{Ca}^{2+}]$, $[\text{Mg}^{2+}]$, $[\text{Na}^+]$, $[\text{K}^+]$, $[\Sigma^+]$, and $[\text{Cl}^-]$ maps of the Efri Haukadalsá	page 21
Fig. H.1: $\delta^{34}\text{S}_{\text{SO}_4}$ of samples collected on a single day throughout the Efri Haukadalsá ...	page 23
Fig. J.1: Rayleigh model calculations	page 26

Appendix A. Images of the Efri Haukadalsá catchment

Images of the Efri Haukadalsá catchment were collected by drone (Fig. A.1), hand-held photography (Fig. A.2), and satellite (Fig. A.3).

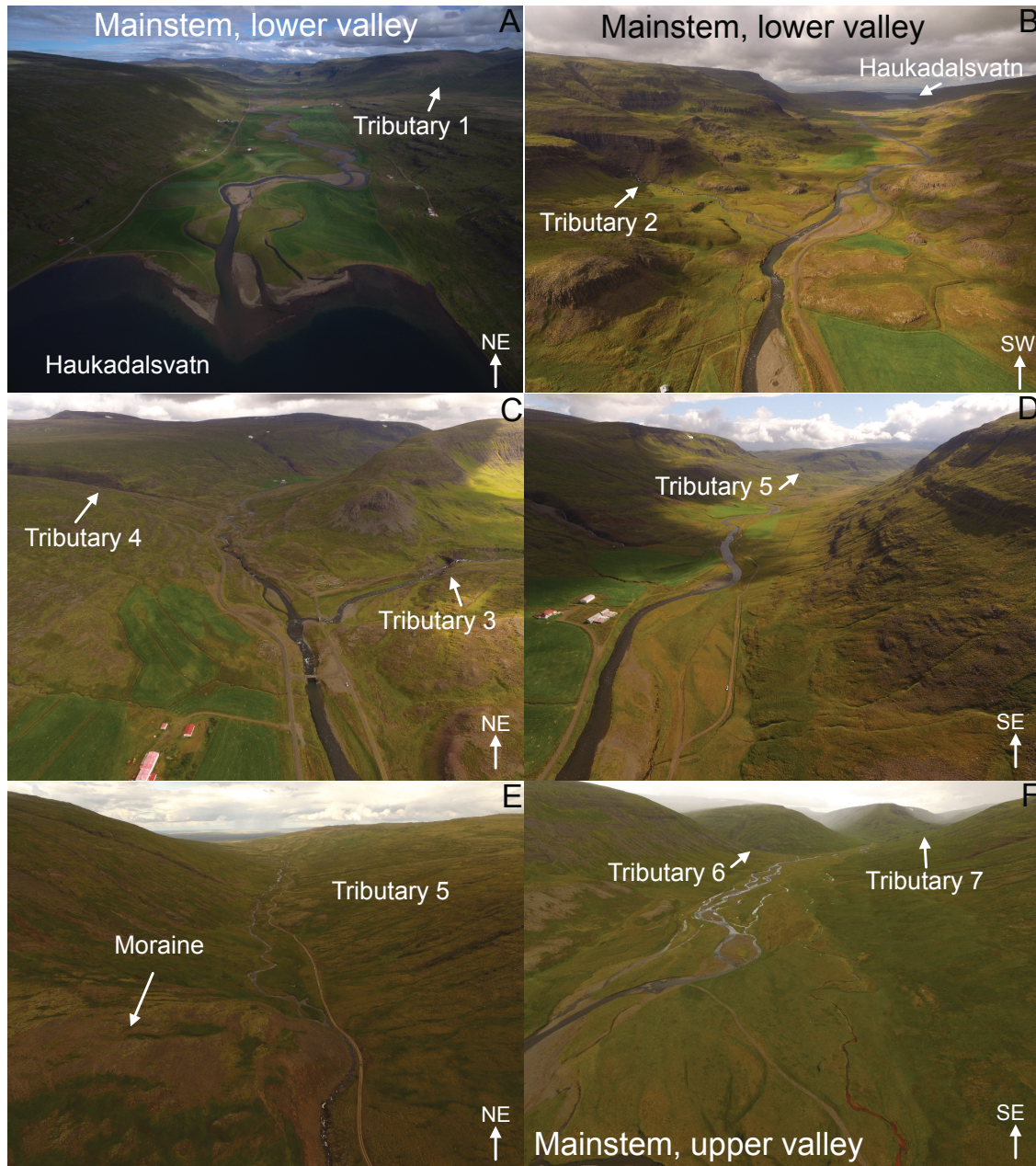


Fig. A.1. Drone images of the Efri Haukadalsá catchment. (A) The lower valley of the catchment viewed from the mouth of Haukadalsvatn and (B) from slightly upstream of the confluence with tributary 2. (C) Confluence of tributary 3 with the Efri Haukadalsá, with tributary 4 also visible. (D) The Efri Haukadalsá between the two knickzones. (E) Tributary 5, which partially drains the moraine. (F) The upper valley of the catchment, with tributary 6 and tributary 7 visible. Arrows in bottom right of each panel indicate approximate image orientation.

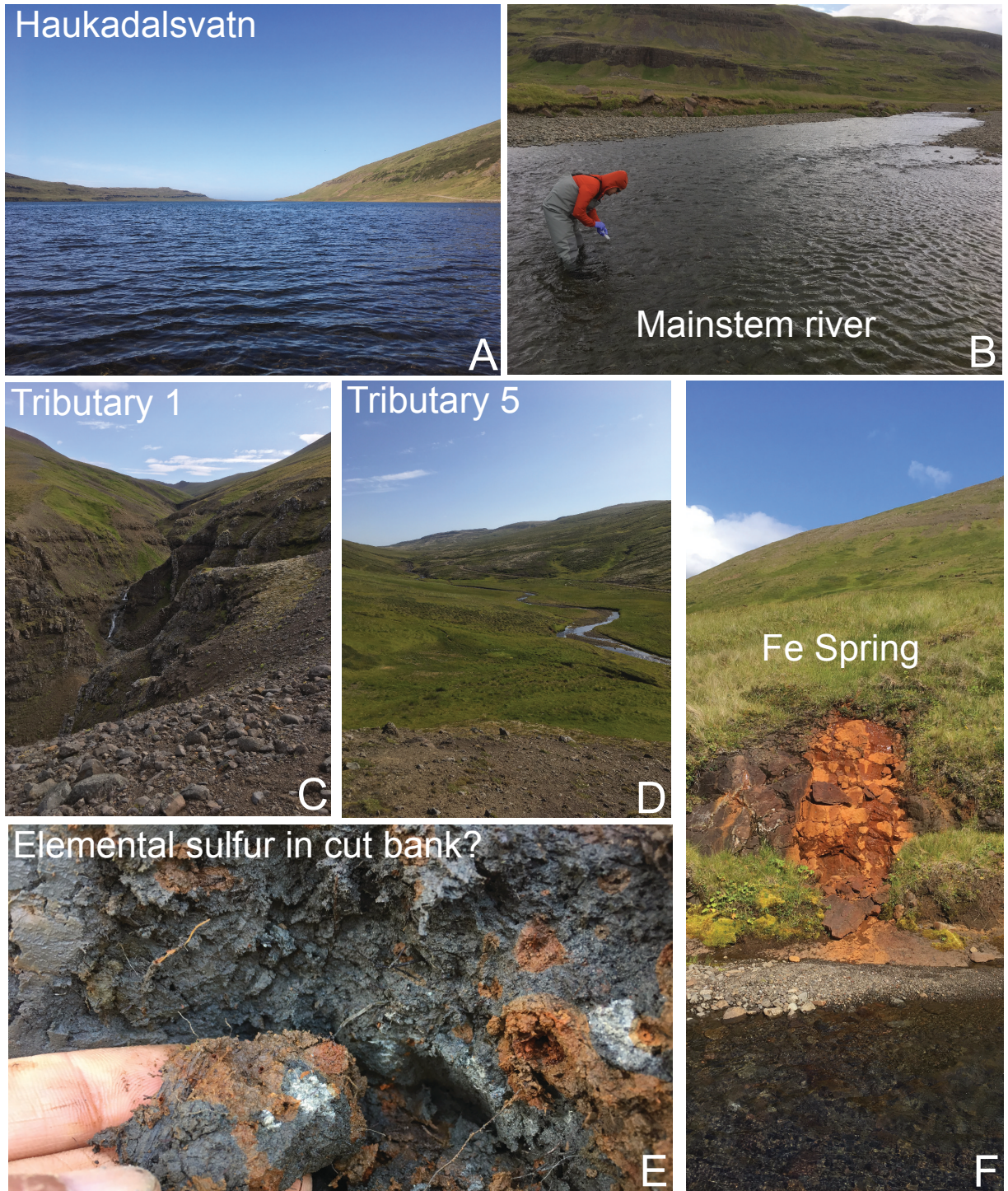


Fig. A.2. Photographs of the Efri Haukadalsá catchment. (A) Lake Haukadalsvatn viewed from the junction with the Efri Haukadalsá. (B) Collecting a water sample from the mainstem river. The person in this image is ~ 2 m tall. (C) Tributary 1, several hundred meters upstream of the confluence with the mainstem. (D) Tributary 5, as seen from the moraine. (E) The smell of white material observed in a cutbank of the lower valley suggested sulfur, but this was not experimentally confirmed. (F) Example of a Fe spring, which are found throughout the Efri Haukadalsá catchment.

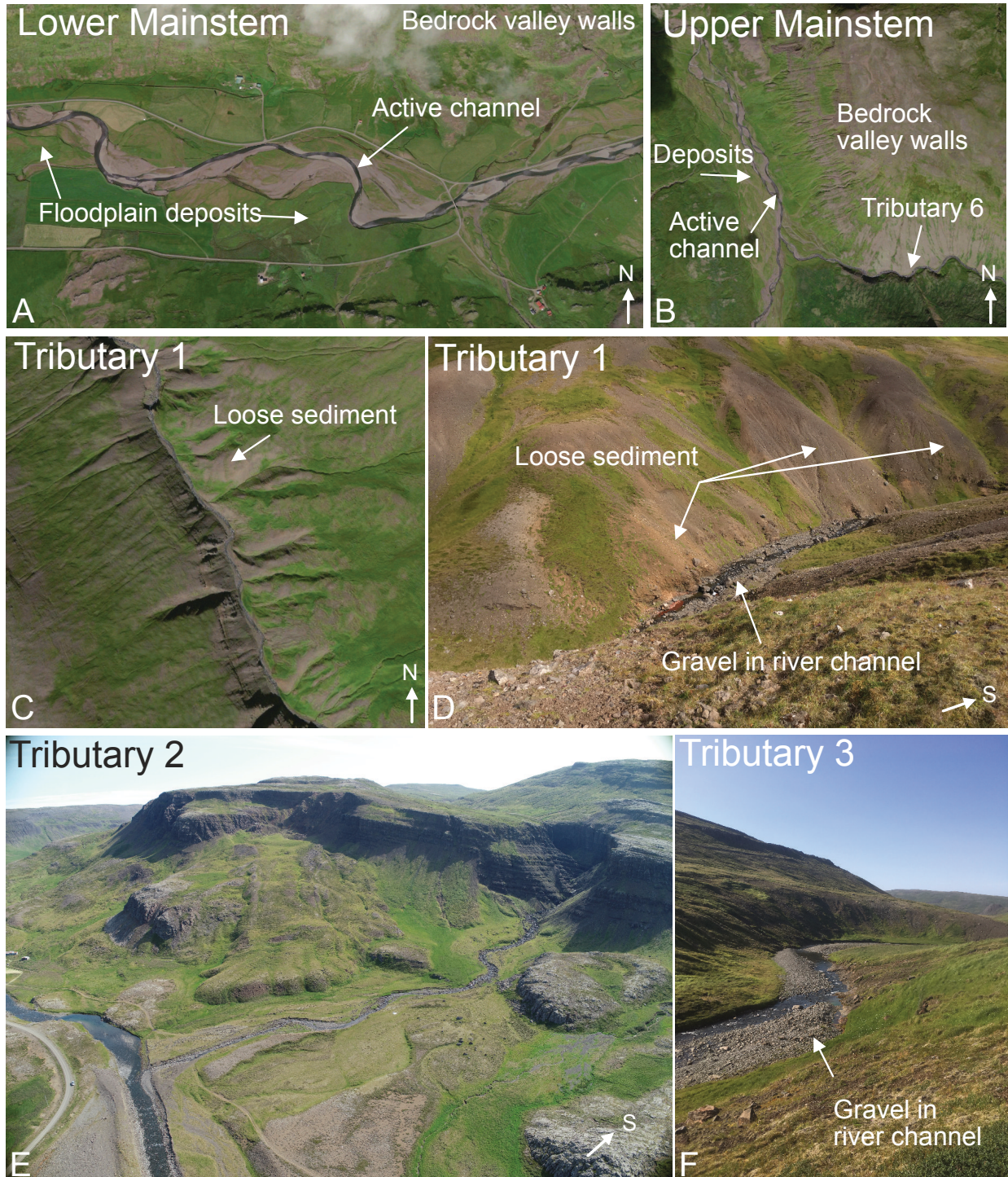


Fig. A.3. (A, B, C) Satellite images from Google Earth and (D, E, F) drone and hand-held photographs of tributaries in the Efri Haukadalsá catchment. (A) The lower mainstem river with floodplain deposits and bedrock valley walls. In this reach the Efri Haukadalsá is a meandering, alluvial river with wide floodplain disconnected from bedrock sources. (B) The upper mainstem river. (C) Satellite and (D) hand-held photograph of tributary 1 with loose sediment and gravel in the river channel. (E) Drone photograph of tributary 2 and (F) hand-held photograph of tributary 3. Arrows in the bottom-right of each panel indicate approximate image orientation.